Three-dimensional metrology of embedded microfeatures in ceramics by infrared optical coherence tomography – advantages and limitations

Rong Su[1,*], Mikhail Kirillin[2], Peter Ekberg[1], Lars Mattsson[1]
1 Department of Production Engineering, KTH Royal Institute of Technology, 68 Brinellvägen, Stockholm 10044, Sweden
2 Laboratory of Biophotonics, Institute of Applied Physics, 46 Ulyanov str., Nizhny Novgorod 603950, Russia

**corresponding author: rongs@kth.se*

Abstract

Advanced printing, structuring, and lamination technologies allow for large-scale and cost-effective manufacturing of multi-layered ceramic micro devices with complex three-dimensional (3D) structures. Infrared (IR) optical coherence tomography (OCT) is a promising technology for rapid, non-contact, high-resolution, and 3D inspection of the microchannels, metal prints, defects, and delaminations embedded in alumina and zirconia ceramic layers at hundreds of micrometres beneath surfaces. In this study the recent progresses of OCT technology for ceramic materials are reviewed, and its advantages and limitations as a metrology tool are evaluated through experiments and Monte Carlo simulations. Several measurement errors of OCT are revealed and the measurement in lateral directions is significantly affected by scattering in the ceramics. Besides of that, two types of image artefacts are found to be present in OCT images due to multiple reflections between neighbouring boundaries and inhomogeneity of refractive index. A wavefront aberration exists in the OCT system with a scanning scheme of two galvo mirrors.

1 Introduction

1.1 Background

The market of multi-functional ceramic micro devices with complex three-dimensional (3D) structures is emerging [1]. Recent progress in advanced manufacturing process allows for massive and cost-effective production of products such as micro-fluidic devices for medical applications or micro-reactions, integrated devices packaged with embedded micro-electro-mechanical systems (MEMS) and optical fibres, bio-reactors, microwave devices for terahertz applications, high-efficiency cooling systems, micro sources of energy, and different types of sensors. Ceramics such as alumina and zirconia are selected as the basic building materials because of their low cost and that they have unique properties of high thermal and chemical stability, mechanical and electrical strength, and electric resistivity [1].

On the other hand quality of the product is a key. As the advanced manufacturing process allows us to build very complex 3D structures inside the material, we are no longer satisfied with measurement of the outer surface of an object. The embedded features become more and more important to be measured, such as geometric dimensions of the machined or printed micro parts inside the material, embedded defects, cracks, voids, delaminations, and inclusions. Thus, a non-destructive, non-contact, high-resolution, and high-speed 3D monitoring systems for quality inspection and process control is highly demanded.

Due to the strong scattering in ceramic materials conventional optical measurement techniques fail to verify the embedded features and detect the defects without significant errors. Ultrasonic testing that requires a liquid couplant between the transducer and the material may lead to a contamination risk [2]. X-ray computed tomography (XCT) with micrometre resolution is a powerful imaging technique [3], but the data acquisition time required for good signal-to-noise ratio (SNR) is too long to be realistic for in-process metrology, and the high X-ray dose may cause lattice defects in ceramic materials and leads to colorations of the materials [4]. Recent development of mid-IR transmission imaging techniques allows for non-destructive optical inspection of zirconia components up to 3.5 mm thick with an imaging resolution of approximately 30 μm [5]. Terahertz imaging which operates between microwaves and far-infrared wavelength region [6] may offer good penetration depth and depth resolution (10 μm may be achieved) in ceramics, but the lateral resolution which is limited by diffraction is usually a few hundred micrometres or in millimetre range.

The most promising technology for this difficult task is optical coherence tomography (OCT) [7]. This technology provides contactless, non-destructive, high-resolution tomographic images based on the low-coherence reflectometry measurement of the “echoes” of backscattered light from internal microstructures within an object. The signal acquisition rate of OCT is excellent and has achieved the level of megahertz today [8]. As a tomographic imaging modality, a series of 1-D longitudinal (depth) scans similar to ultrasound A-scans are performed pointwise along a line in the lateral x-direction. By

combining these scans for a given y-position a 2-D cross-sectional image is obtained (analogous to the ultrasonic pulse-echo imaging B-scan). By further combining these cross-sectional images recorded at adjacent y-positions a full 3-D tomographic image can be obtained.

1.2 Review of OCT measurement in ceramics

Although OCT was originally developed as an imaging technology in biomedicine for tissues such as the eye, arteries, and nervous tissues [7], new applications have appeared in recent years into the fields of dimensional metrology, material research, non-destructive testing, art diagnostics, botany, microfluidics, data storage, and security applications [9].

Early applications of OCT in ceramics were investigated by Bashkansky et al. [10, 11], including materials such as lead zirconate titanate (PZT), silicon nitride ceramics, single-crystal silicon carbide and Teflon-coated wires. Later Veilleux et al. [12] used OCT B-scan images to evaluate the light penetration depth inside plasma-sprayed yttria-stabilized zirconia (YSZ) coatings and determined the refractive index of the material. Sinescu et al. [13] evaluated the potential of en-face OCT for assessing the ceramic material defects of dental prostheses and micro-leakage at prosthetic interfaces, as well as the quality of bracket bonding on dental hard tissue. Gaps between the dental interfaces and ceramic material defects were clearly exposed in the B-scan and volumetric OCT images. Ellingson et al. [14] used OCT to measure the thicknesses of thermal barrier coatings (TBCs) that usually consist of YSZ and are used in gas turbine engines for preventing damages to the substrate materials. Recently, Su et al. [15-17] modified the scattering model of sintered alumina and zirconia ceramic materials for accurate Monte Carlo simulation of OCT images, and thoroughly investigated the feasibility of mid-IR OCT for improvement of penetration depth in the ceramics.

The major limitation of the quality of OCT images is speckles caused by the coherent nature of light. The SNR may be close to or even smaller than “1” in an image [18]. Therefore, surface recognition and segmentation in OCT images remains a challenge. Su et al. [19] developed an automated 3D image processing algorithm with sub-pixel resolution for improving the accuracy of the dimensional measurement from OCT data of industrial ceramic samples.

1.3 Problem

The major problem with regard to the dimensional metrology and defect detection using OCT in ceramics is the limited penetration of radiation due to strong scattering and the un-known measurement errors. The answer to the former may be an OCT system using a mid-IR supercontinuum light source and high quality cooled super-lattice photon detectors [16]. However, to the best of our knowledge the measurement errors of OCT have not been studied systematically. This problem will be discussed in this paper.

2 Principle of OCT

The fundamental principle of OCT technology is based on the interference of partially coherent electromagnetic waves. The standard time-domain OCT layout is shown in Figure 1. The key component is the broadband source (or femtosecond laser) that works in IR region. The radiation emitted from a broadband source is sent into the Michelson interferometer and divided into a reference beam and a sample beam.

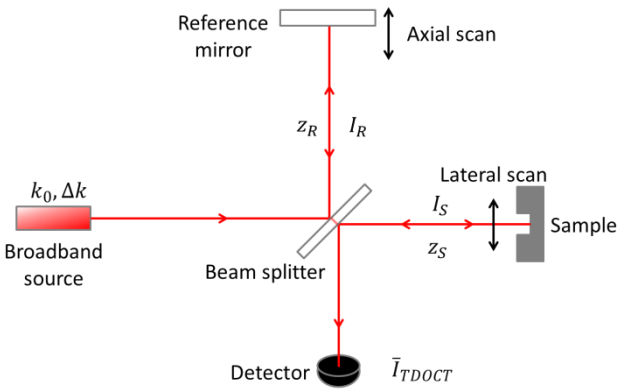

Figure 1: Schematics of the standard time-domain OCT setup

The reference beam reflected back from a mirror interferes with the sample beam backscattered from the sample at the beam splitter, and then the interference signal is detected by the detector and can be expressed as below (if Gaussian-distributed spectrum of the source is assumed)

$$\bar{I}_{TDOCT} \sim I_R + I_S + \sqrt{I_R I_S}\; e^{-\Delta k^2 (z_R - z_S)^2} \cos[2k_0(z_R - z_S)]$$

where I_R and I_S is the intensity of the reference beam and sample beam, respectively. k_0 is the spatial frequency corresponding to the centre wavelength, and Δk is the spectral width. z_R and z_S are the optical pathlengths of the reference beam and the sample beam, respectively. The interference signal occurs only when $(z_R - z_S)$ is small enough, usually in the order of a few micrometres for a modern OCT system. By scanning the reference mirror axially a depth-resolved A-scan is obtained. A 3D volumetric image can be obtained by laterally scanning the sample beam using two galvo mirrors with rotational axes in x- and y-direction.

More advanced Fourier-domain OCT (FD-OCT) also relies on the principle of partially coherent interference, but it offers a possibility of much faster imaging speed and higher detection sensitivity. Instead of mechanically scanning a reference mirror an A-scan is obtained by a Fourier transform of the spectrally resolved interference fringes. This can be done by using a spectrometer as detector, e.g. a line array charge-coupled device (CCD). Such a

system is called spectral-domain OCT (SD-OCT). It can also be done by employing a swept laser source (wavelength-tuning) with a single photodetector to record the spectrally resolved interferogram sequentially while tuning the wavelength. This is called swept-source OCT (SS-OCT). The same underlying principle is used in both methods, i.e. to reconstruct the coherence function by calculating the Fourier transform of the measured power spectrum. The detailed explanation of this technique is skipped here but can be found in [7].

3 Experimental

The sintered highly-dense polycrystalline alumina and zirconia ceramic materials are investigated. The samples are made in thin layers (thickness of 50-500 µm) and have white appearance due to high scatter [17]. Laser milling technology is used for structuring the ceramic layers. The sample under test is a two-layer ceramic stack with embedded laser-milled channels as shown in Figure 2. The imaging sites are marked with the red frames.

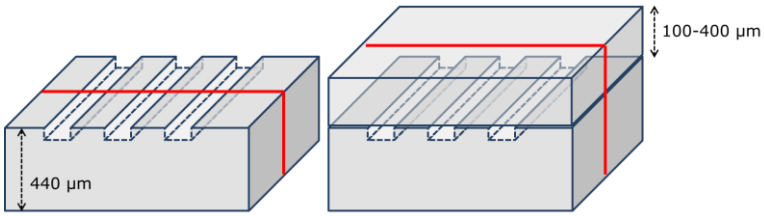

Figure 2: Geometric model of the two-layer ceramic sample stack

The OCT systems used in this study include a commercial spectral-domain OCT and two laboratory swept-source OCT systems [20]. The specifications of the systems are given in Table 1.

Table 1: Specifications of the OCT systems

	Commercial system	Laboratory systems	
Centre wavelength	1325 nm	1300 nm	1650 nm
Maximum A-scan rate	91 kHz	10 kHz	10 kHz
Lateral resolution	15 µm	< 20 µm	< 20 µm
Axial resolution	< 8 µm	< 20 µm	< 20 µm

The Monte Carlo simulation program used in this study has been developed and tested in previous studies [16]. The simulations of OCT images are carried out by a consecutive step-wise calculation of individual A-scans that are further combined into a 2D matrix and displayed as an image in a logarithmic scale. Surface roughness was included as a parameter in the simulation.

4 Result

4.1 OCT measurement of ceramics

The 3D OCT image of the two-layer zirconia ceramic stack is demonstrated in Figure 3. The microchannels are covered by a 375 µm thick zirconia layer. The top and the bottom surfaces of the channels can be clearly detected. The image covers a volume of 4mm×4mm×1.78mm, where the vertical axis presents optical distance.

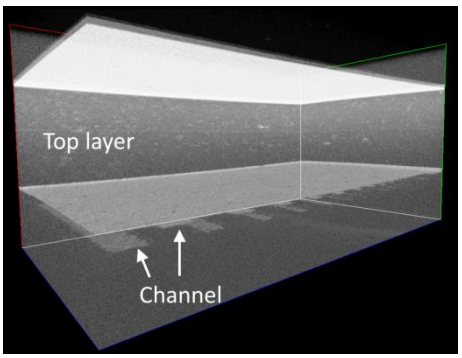

Figure 3: The 3D OCT image of the two-layer ceramic stack

By analysing the 3D OCT data using our image processing algorithm [19] the channel surfaces are segmented and displayed as the top-view OCT images in Figure 4. The field of view (FOV) is 4 mm × 4 mm. From this result the heights and widths of the channels can be easily obtained.

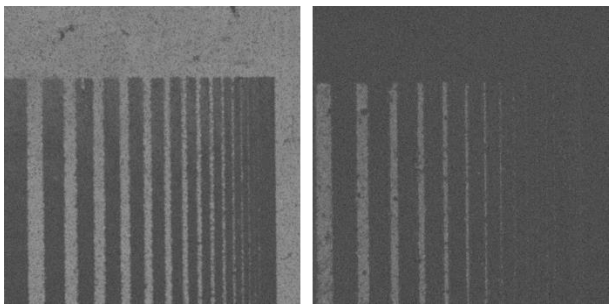

Figure 4: Top-view OCT images of the top and bottom surfaces of the channels

Air-filled pores with diameters larger than 10 µm may become the starting points of potential cracks in the material. They are present in OCT images as extraordinary bright spots as shown in Figure 5.

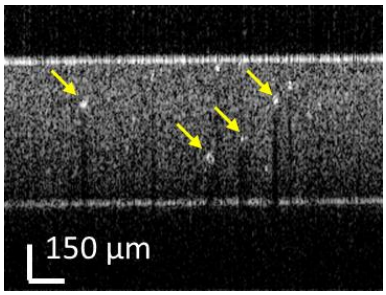

Figure 5: Cross-sectional OCT images of a sintered zirconia layer

Delamination between two stacked ceramic layers may happen in the sintering process. The delamination is observed as separated interfaces in the OCT image as shown in Figure 6. The detectable separation is smaller than 10 µm owing to the high axial resolution.

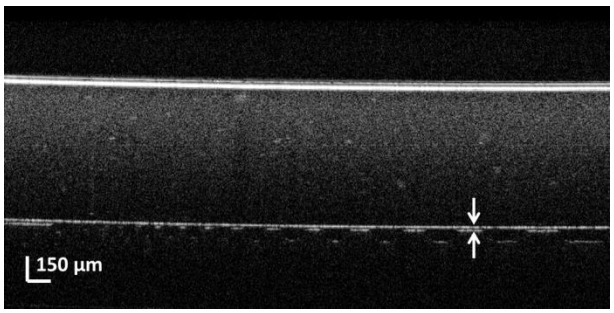

Figure 6: Cross-sectional OCT image of the embedded microchannels

4.2 limitation of OCT imaging in ceramics

The primary limitation of OCT imaging in ceramics is the penetration depth. This may be improved by operating OCT in mid-IR. The Monte Carlo simulation predicts the expected OCT response in the near to mid-IR wavelength regions. The details of the simulation can be found in [16]. The simulated cross-sectional OCT images based on the experimental geometric model are shown in Figure 7 at five different wavelengths. Surface roughness and dispersion effect have been taken into account in the simulation. It is obvious that the penetration depth is improved with increasing wavelength. The image contrast of the embedded channel is considerably enhanced. The vertical axis represents the optical distance and the color-coded calculated intensity corresponds to a dynamic range of 55 dB. A mirrored image artefact of the channel surface (s3) is present in Figure 7E as the penetration depth is improved. This is because some photons are reflected twice between the surfaces s2 and s3. Another phenomenon is the distorted image of the flat s4 as observed in Figure 7D and Figure 7E. An inverted channel appears in the image instead of a straight

line because the photons passing through the air-filled channel have travelled a shorter optical pathlength to reach and return from this boundary at the channel region.

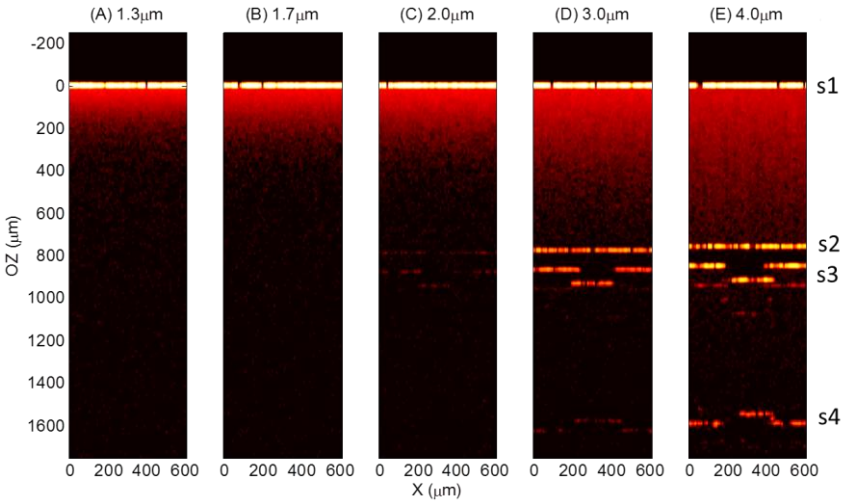

Figure 7: Simulated OCT images of the two-layer alumina stack

The OCT measurement has been found accurate in axial direction for a measurement of embedded structures in the axial direction [15], but can be problematic for the measurement in the lateral X- and Y-directions. As shown in Figure 8 four channels with different widths are measured in free surface and embedded in 188 µm thick alumina and 375 µm thick zirconia layers, respectively. The deviations of the measured widths are almost constant between the embedded channels and those in free surface. This is probably caused by a reduced OCT signal from the channel edges owing to the strong scattering that occurs in the top alumina or zirconia layer, and the presence of surface roughness.

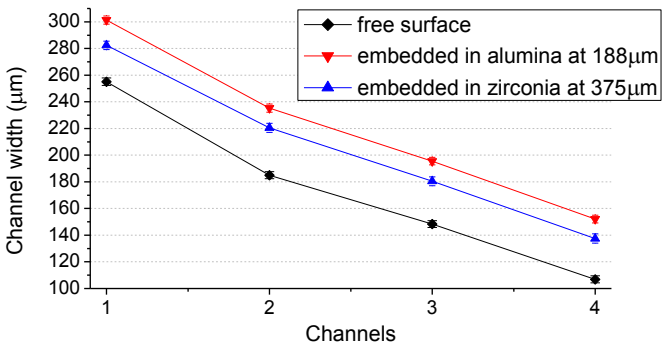

Figure 8: Comparison of the measured widths of four embedded channels

Another problem in OCT imaging is the wavefront aberration caused by the imaging optics, particularly when a pair of galvo mirrors is used for the lateral scanning. This aberration exists in most OCT systems that use this scanning scheme, which is a 3rd-order aberration (astigmatism at zero degree and defocus). For some scanning schemes the peak-to-valley (P-V) error can be as large as some 20 µm over a 4×4 mm^2 FOV. This aberration can be measured and corrected by extracting the OCT image of a flat surface using a dedicated 3D image processing algorithm [19]. The actual wavefront error is demonstrated in Figure 9 and the colour bar corresponds to height values in micrometres.

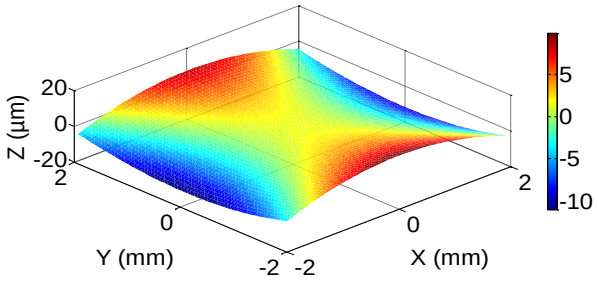

Figure 9: Plot of the wavefront aberration of an OCT system

5 Conclusion

Optical coherence tomographic method is promising for inspection and metrology of embedded structures in multi-layered alumina and zirconia ceramics. By Monte Carlo simulation of OCT images we find the optimal OCT wavelength region is 2-4 µm for alumina and zirconia ceramic materials, and surface roughness may degrade the detectability of the embedded interfaces in materials. On the other side, we investigated and revealed some of the limitations of OCT from the metrology point of view. The measurement of the width of the embedded channel is significantly affected by scattering in the ceramics. The result also shows image artefacts may cause severe inspection errors, particularly for unexperienced operators. Our dedicated Monte Carlo simulation program and 3D image processing algorithm may significantly enhance the understanding of the imaging mechanism and improve the accuracy and precision of the OCT inspection and measurement.

Reference

[1] MULTILAYER, EU FP7 project, http://multilayer.4m-association.org/.
[2] Birks A and Green R 1991 *Ultrasonic Testing 2nd ed* (Columbus)
[3] Stock S 2008 *MicroComputed Tomography: Methodology and Applications* (CRC Press)
[4] Evans B D and Stapelbroek M 1978 *Phys. Rev.* B **18** 7089-7098

[5] Matysiak M, Parry J P, Albri F, Crowder J G, Jones N, Jonas K, Weston N, Hand D P and Shephard J D 2011 *Meas. Sci. Technol.* **22** 125502
[6] Chen C, Lee D, Pollock T and Whitaker J F 2010 *Opt. Express* **18** 3477-86
[7] Drexler W and Fujimoto J G 2008 *Optical Coherence Tomography Technology and Applications* (Springer Berlin Heidelberg New York)
[8] Wieser W, Biedermann B R, Klein T, Eigenwillig C M and Huber R 2010 *Opt. Express* **18** 14685-704
[9] Stifter D 2007 *Appl. Phys.* B **88** 337–57
[10] Bashkansky M, Duncan M D, Kahn M, Lewis D III and Reintjes J 1997 *Opt. Lett.* **22** 61-63
[11] Duncan M D, Bashkansky M and Reintjes J 1998 *Opt. Express* **2** 540-45
[12] Veilleux J, Moreau C, Lévesque D, Dufour M and Boulos M I 2006 *Review of Quantitative Nondestructive Evaluation* **25** 1059-66
[13] Sinescu C et al 2008 *J. Biomed. Opt*. **13** 054065
[14] Ellingson W A, Visher R J and Lipanovich R S 2006 *Materials Evaluation*
[15] Su R, Kirillin M, Ekberg P, Roos A, Sergeeva E and Mattsson L 2012 *Opt. Express* **20** 4603-18
[16] Su R, Kirillin M, Chang E W, Sergeeva E, Yun S H and Mattsson L 2014 *Opt. Express* **22** 15804-19
[17] Su R 2014 PhD thesis, KTH Royal Institute of Technology, ISBN 978-91-7595-090-5
[18] Schmitt J M, Xiang S H and Yung K M 1999 *J. Biomed. Opt.* **4** 95-105
[19] Su R, Ekberg P, Leitner M and Mattsson L 2014 *J. Opt. Soc. Am.* **31** 2551-60
[20] Sharma U, Chang E W and Yun S H 2008 *Opt. Express* **16** 19712-23